

Fermi-surface Shrinking, Interband Coupling and Multiple Gaps in Iron-based Pnictides

E. Cappelluti · L. Ortenzi · L. Benfatto

Received: 8 September 2010 / Accepted: 9 September 2010 / Published online: 24 September 2010
© Springer Science+Business Media, LLC 2010

Abstract In this contribution we present a comprehensive explanation for the origin of the band shifts observed in dHvA and ARPES experiments. Using a four-band Eliashberg analysis, we show that they are a natural consequence of the multiband character of these systems and of the strong particle-hole asymmetry of the bands. We also show that the relative sign of such shifts provides a direct experimental evidence of a dominant interband scattering. A quantitative analysis in LaFePO yields a spin-mediated interband coupling of the order $V \approx 0.46$ eV, which corresponds to a mass enhancement $Z \approx 1.4$. We also employ such four-band model to investigate the magnitude of the superconducting gap on different Fermi sheets of $\text{Ba}_{0.6}\text{K}_{0.4}\text{Fe}_2\text{As}_2$, and we show that the same four-band model provides a simple explanation of the different gap values on different Fermi sheets and of the thermodynamics properties (specific heat, superfluid density, ...).

Keywords Pnictides · Multiband superconductivity · Band shifts · Spin-fluctuations

E. Cappelluti (✉) · L. Benfatto
Institute of Complex Systems, CNR, U.O.S. Sapienza, v. dei
Taurini 19, 00185 Rome, Italy
e-mail: emmanuele.cappelluti@gmail.com

E. Cappelluti · L. Ortenzi · L. Benfatto
Department of Physics, University “La Sapienza”, P.le A. Moro 2,
00185 Rome, Italy

Present address:

L. Ortenzi
Max-Planck-Institut für Festkörperforschung, Stuttgart, Germany

1 Introduction

A new challenge in the field of condensed matter is represented by the recent discovery of high- T_c superconductivity in iron-based pnictides [1, 2]. The main object of investigation in this context is, as usual, the determination of the microscopic origin of the scattering mechanisms operative in these systems, and hence of the superconducting pairing. Things are here even more complex, and also interesting, because of the multiband character of these systems. According to Density Functional Theory (DFT) calculations, indeed, the band structure of pnictides near the Fermi level is characterized by two hole-like bands around the Γ point, and two electron-like bands around the M point of the reduced Brillouin zone [3–7]. A third hole-like band at the Γ point could be expected to cross the Fermi level in some materials, but eventually it moves below the Fermi level when the experimental value of the apical As position is used in DFT calculations [8]. The comparison with experimental measurements of electronic excitations with DFT predictions can shed thus a useful insight on the underlying scattering mechanism. In this context a first puzzling feature of these materials is the systematic experimental observation, by using angle-resolved photoemission spectroscopy (ARPES) [9–12] and de Haas-van Alphen (dHvA) [13–15] probes, of relative band shifts when compared with DFT calculations, resulting in corresponding Fermi-surface shrinkings. Quite interesting, such shifts are *band selective*, in such a way that electron-like bands result to be shifted upwards while hole bands are shifted downwards. An additional issue concerns the experimental observation of only two gap-values in hole-doped 122 compounds [9, 16], whereas in a multiband BCS approach one would generically expect a different gap value in each band, depending on the coupling and on the density of states (DOS) of the several pockets involved in the pairing. Further difficulties arise in the

attempt to reconcile ARPES data with several thermodynamic measurements. For instance, photoemission experiments performed by several groups in different pnictide materials have shown that there is a substantial renormalization of the whole band structure with respect to DFT predictions, with a reduction at least of a factor two [9–12, 17, 18]. At the same time, the estimates of the specific-heat coefficient C_V/T obtained by using the ARPES bandwidth, despite being substantially larger than DFT, are still about a factor two smaller than the values measured in the normal state for 122 compounds [19–21]. This comparison calls for a dichotomy between high-energy and low-energy mass renormalization, which must be accounted for by different mechanisms.

In this contribution we employ a four-band Eliashberg analysis to provide a systematic analysis of spectral and thermodynamic properties in pnictides with the goal of reconciling the results obtained with the different probes. We show that the observed bands shifts, and the corresponding Fermi-surface shrinking, can be natural explained as result of the strong particle-hole asymmetry of the bands, which induces finite-band self-energy effects [22]. The particular sign of the band shift of the hole and electronic sheets provides a direct evidence of a dominant *interband* scattering. Our calculations give an estimate the interband coupling $V \sim 0.46$ eV in undoped LaFePO [22]. We also show that the spectroscopic and thermodynamic properties of optimally doped $\text{Ba}_{0.6}\text{K}_{0.4}\text{Fe}_2\text{As}_2$ (BKFA) can be also accounted for in the four-band Eliashberg analysis, using high-energy electronic dispersion taken from the experiments, with dimensionless coupling $\lambda \sim 0.2$ and $\lambda \sim 1.6$ depending on the band [23].

2 Band Shifts in LaFePO

The physical properties of pnictides are analyzed within a four-band Eliashberg analysis. Using the Nambu notation, we can write a self-consistent equation for the self-energy:

$$\hat{\Sigma}_\alpha(i\omega_n) = -\pi T \sum_{\beta, m} V_{\alpha, \beta} D(\omega_n - \omega_m) \hat{G}_\beta(i\omega_m), \quad (1)$$

where α, β are band indices, $V_{\alpha, \beta}$ is the multiband interaction, and $D(\omega_n - \omega_m)$ is the boson propagator, which is related to the Eliashberg function $B(\Omega)$ by $D(\omega_n - \omega_m) = \int 2\Omega d\Omega B(\Omega)/[(\omega_n - \omega_m)^2 + \Omega^2]$. In addition, $\hat{G}_\alpha(z)$ is here the 2×2 local Green's function for the α band, namely

$$\hat{G}_\alpha(i\omega_n) = \sum_{\mathbf{k}} \frac{1}{(i\omega_n + \mu)\hat{\tau}_3 - \varepsilon_{\mathbf{k}, \alpha}\hat{\tau}_3 - \hat{\Sigma}_\alpha(i\omega_n)}, \quad (2)$$

and $\hat{\tau}_i$ are the Pauli matrices in Nambu space. Decomposing the self-energy in its Pauli components, $\hat{\Sigma}_\alpha(i\omega_n) = \sum_{i=0, \dots, 3} \Sigma_\alpha^i(i\omega_n)\hat{\tau}_i$, we can obtain the renormalization fac-

tor Z_α for each band as $Z_\alpha = 1 - \Sigma_\alpha^0(i\omega_{n=0})/\pi T$, while the superconducting gaps Δ_α are obtained as $\Delta_\alpha = \phi_\alpha/Z_\alpha$, where $\phi_\alpha = \Sigma_\alpha^2(i\omega_{n=0})$. Finally, the self-energy component $\propto \hat{\tau}_3$, namely $\chi_\alpha = \Sigma_\alpha^3(i\omega_{n=0})$, gives rise to a *band-selective* shift for the dispersion of the band α . This contribution is neglected in the standard Eliashberg theory, where, as we show below, the infinite bandwidth approximation enforces the particle-hole symmetry. For the moment we shall focus on the relevance of this latter feature, and we consider the normal state.

In order to gain a qualitative insight on the physical origin of such shift, it is instructive to consider the lowest order perturbation theory where the Green's function in (1) is taken to be the non-interacting. We consider for simplicity two-dimensional parabolic bands with $\varepsilon_{\mathbf{k}, \alpha} \in [E_{\min, \alpha} : E_{\max, \alpha}]$, which for pnictides is a good approximation. In the adiabatic limit $\omega_0 \ll |E_{\max, \alpha}|, |E_{\min, \alpha}|$ we can write

$$\chi_\alpha \approx -\frac{\omega_0}{2} \sum_{\beta} V_{\alpha, \beta} N_\beta \ln \left| \frac{E_{\max, \beta} - \mu}{E_{\min, \beta} - \mu} \right|, \quad (3)$$

where $N_\alpha = 1/(E_{\max, \alpha} - E_{\min, \alpha})$ is the DOS of the α band.

It is now easy to see that in the infinite bandwidth approximation, as well as in any case where the particle-hole symmetry is present, $|E_{\max, \alpha} - \mu| = |E_{\min, \alpha} - \mu|$ so that $\chi_\alpha = 0$. Equation (3) shows also another interesting result, namely that the *sign* of the band shift χ_α depends on the overall electron-like or hole-like character of the bands β coupled to the band α . This is particularly important in iron-based pnictides where, due to the nesting properties, the dominant coupling is thought to be the spin-mediated interband interaction. In such a situation, the particle-hole asymmetry of the electron bands is responsible for the downward shift of the hole-like bands, which, vice versa, give rise to the upward shift of the electron ones. In full generality we can thus say that *the simple observation of a upward shift of the electron bands and the downward shift of the hole-like ones is direct experimental evidence in these compounds of the dominance of the interband coupling on the intraband one.*

We can employ this analysis to get a more quantitative insight on LaFePO where detailed measurements of the band shifts by means of dHvA techniques have been reported. We consider four bands and we assume, because of the nesting properties, a purely interband scattering connecting hole-like and electron-like bands, as depicted in Fig. 1a. Since in LaFePO all the Fermi areas are roughly comparable, we assume as a first approximation $V_{1,3} = V_{1,4} = V_{2,3} = V_{3,4} = V$ [22]. To account for a spin-mediated interaction mechanism we use the Lorentzian spectrum typical of spin fluctuations [24] $B(\Omega) = \Omega\omega_0/\pi(\omega_0^2 + \Omega^2)$ with the characteristic energy scale $\omega_0 = 20$ meV. We model each band with a purely two-dimensional parabolic dispersion $\varepsilon_\alpha(\mathbf{k}) = \varepsilon_\alpha^0 - t_\alpha |\mathbf{k}|^2$, where \mathbf{k} is measured with respect

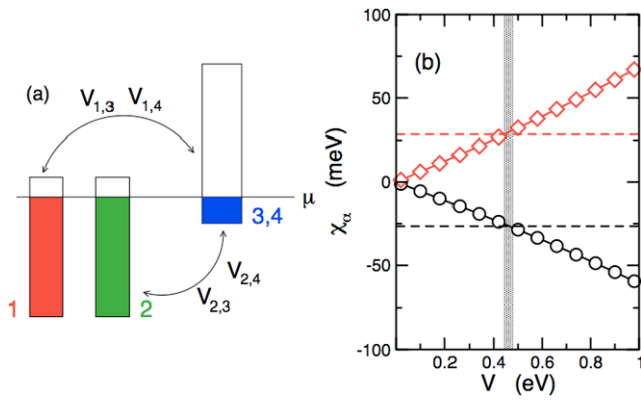


Fig. 1 (a) Sketch of our band structure model. (b) Band shifts χ_α as functions of the interband coupling V . The horizontal dashed lines mark the average band shift as would be estimated in [13, 14] using the renormalized bands, the vertical grey region the estimate coupling $V \approx 0.46$ eV

Table 1 Microscopic band parameters extracted from DFT calculations after a band structure renormalization by a factor 2. Also shown, in the last two columns on the right, the calculated band shifts χ_α and the renormalized mass m_α^* for $V = 0.46$ eV. m_e is the free electron mass

Band	$E_{\max,\alpha}$ (eV)	$E_{\min,\alpha}$ (eV)	N_α (eV ⁻¹)	χ_α (meV)	m_α^*/m_e
1	0.102	-2.516	0.382	-26.5	1.6
2	0.102	-1.231	0.750	-26.5	3.2
3, 4	1.776	-0.147	0.529	31	2.3

to the Γ point for the hole bands and to the M point for the electron bands. $N_\alpha = 1/4\pi t_\alpha$ is thus the DOS (per spin) in each band. A debated issue in this context is the assessment of a proper choice for the underlying normal-state electronic bands. Indeed, as we mentioned in the introduction, ARPES measurements in several pnictide families report significant differences in the electronic dispersion compared with DFT calculations, with an apparent renormalization of the whole band structure by a factor 2 [9–12, 17]. Most striking, such band narrowing seems to be operative up to very high energy scales, as it is confirmed also by recent optical sum-rule analysis performed in LaFePO samples [25]. This overall renormalization of the bands with respect to DFT seems thus a general feature of pnictides, probably arising from local Hubbard-like correlations [26–28], so that it cannot be captured by the coupling of the electrons to low-energy bosonic modes. To take into account this feature, we extract the band parameters from the DFT calculations [3], and we renormalize the electronic energy scales by a factor 2 in agreement with the experimental band structure observed by ARPES [17]. All the estimated values are reported in Table 1.

In Fig. 1b we show the band shifts χ_α evaluated from the numerical solution of (1)–(2) as a function of V . Note that, since we are considering $V_{\alpha,\beta} = V$, the band shift of the two different hole bands is equal $\chi_1 = \chi_2$, as well as

for the two electron bands. From Fig. 1b we get an estimate $V \approx 0.46$ eV to account for the hole band shift $\chi_{1,2}^{\text{exp}} \approx -26.5$ meV needed to reproduce the experimental Fermi area with the renormalized band structure. With these values we obtain a multiband coupling matrix where $\lambda_{1,3} = \lambda_{1,4} = \lambda_{2,3} = \lambda_{2,4} = 0.24$, $\lambda_{3,1} = \lambda_{4,1} = 0.18$, $\lambda_{3,4} = \lambda_{4,2} = 0.34$ and zero otherwise [22]. With these values we also get $T_c \sim 9$ K in good agreement with the experimental value $T_c^{\text{exp}} \sim 6$ K. The total coupling per band is roughly isotropic $\lambda = \sum_\beta \lambda_{\alpha,\beta} \approx 0.48\text{--}0.52$, in the weak-coupling regime. With these values we can compute the mass renormalization factor $Z_\alpha \approx 1.5$ and the specific heat per unit cell $\gamma = \sum_\alpha (\pi/3\hbar^2) m_\alpha Z_\alpha k_B^2 a^2 N_A$, where k_B is the Boltzmann constant, N_A the Avogadro number and $a = 3.9$ Å. We thus obtain $\gamma = 14.1$ mJ/mol K² also in good agreement with experimental estimates $\gamma = 11\text{--}14$ mJ/mol K² [29–31].

3 Superconducting and thermodynamic properties of BKFA

We can now employ the four-band Eliashberg framework to analyze the spectral and thermodynamical properties of the superconducting state of optimally doped BKFA. In this case, because of the different size of the inner and outer hole-like Fermi surfaces, denoted respectively as band 1 and 2, we could expect a significant difference, due to the different nesting properties, for the corresponding couplings with the two degenerate electron bands. We denote thus $V_{1,3} = V_{1,4} = G$ and $V_{1,3} = V_{1,4} = g$. We estimate the band-structure parameters directly from ARPES experiments [9], as listed in Table 2. The different values of DOS in each band are expected to give rise, in a weak-coupling BCS analysis, to three different values of the superconducting gaps on the two hole pockets and on the electron bands, respectively. The experimental observation from ARPES of two nearly degenerate gaps on the hole band 1 and on the electron bands 3–4 signalizes thus the relevance of a strong coupling interaction, as discussed in [32] for a two-band model and in [23, 33] for a four-band model in the explicit case of optimal doped BKFA. In particular, the experimental value of the Δ_α on each band can be used as an input constraint to determine qualitatively the unknown value of the interband interaction. In Table 2 we summarize our results for the interband scattering $G = 1.1$ eV, $g = 0.35$ eV obtained to reproduce the experimental gaps. The multiband matrix of the coupling constants reads in this case $\lambda_{1,3} = \lambda_{1,4} = 0.55$, $\lambda_{2,3} = \lambda_{2,4} = 0.18$, $\lambda_{3,1} = \lambda_{4,1} = 1.62$, $\lambda_{3,4} = \lambda_{4,2} = 1.01$ and zero otherwise [23]. We obtain a critical temperature $T_c = 48.7$ K, which overestimates the experimental one $T_c^{\text{exp}} \sim 37$ K. One should consider, however, that superconducting fluctuations, which are not taken into account in the present analysis, are expected to decrease the critical temperature.

Table 2 Microscopic band parameters extracted from [9] by approximating each band with a parabolic form $\varepsilon_i(\mathbf{k}) = \varepsilon_i^0 - t_i|\mathbf{k}|^2$. $N_i = 1/4\pi t_i$ is the DOS (per spin) in each band. Also shown are the physical properties Δ_i , Z_i , m_i^*/m_e and $J_{s,i}$ evaluated within the four-band Eliashberg theory

Band	ε_α^0 (meV)	t_α (meV)	N_α (eV $^{-1}$)	Δ_α (meV)	Z_α (eV $^{-1}$)	m_α^*/m_e	$J_{s,\alpha}(0)$ (meV)
1	28	54	1.47	9.48	2.09	9.61	4.8
2	43	27.5	2.89	4.35	1.35	12.28	10.7
3, 4	-60	160	0.50	-10.48	3.67	5.72	6.14

The qualitative determination of the multiband scattering matrix can be now employed to investigate further superconducting and normal-state properties. A first important issue concerns for instance the quasi-particle renormalization factors Z_α , which are connected to the mass enhancements $m_\alpha^*/m = Z_\alpha$. Different experimental methods are available to detect these features. On one hand, such mass enhancements are operative only below the spin-fluctuation energy scale ω_0 , so that they are expected to give rise a remarkable kink at this energy [23]. On the experimental ground, however, the experimental resolution of the data in [9] is unfortunately not high enough to resolve the effect of low-energy spin fluctuations from the high-energy renormalization (it is interesting to notice that a similar kink has been actually observed [34] in high-resolution ARPES measurements performed by another group in a BKFA sample with lower doping than the one we are discussing here). On the other hand, the signatures of low-energy renormalization are much more easily detectable in thermodynamic measurements of mass enhancement than in photoemission, where a very high resolution is required to resolve the kinks in the band dispersion. A powerful tool in this perspective is for instance the analysis of the specific heat γ_N in the normal state. Within DFT one obtains $\gamma_N = 9.26$ mJ/K 2 mol [35], that is remarkably smaller than the values of γ_N measured in doped BKFA, either by direct analysis of the normal-state specific heat $\gamma_N = 49$ mJ/K 2 mol [21], or by measurements of the upper critical field $\gamma_N = 63$ mJ/K 2 mol [20]. By means of the band parameters extracted from ARPES and listed in Table 2, one thus estimates $\gamma_N = 25$ mJ/K 2 mol in the absence of interaction, while, with the renormalized masses listed in Table 2, which include low-energy renormalization effects on the ARPES bands, we can estimate $\gamma_N = 50$ mJ/K 2 mol, in very good agreement with [21]. Thus, the additional mass renormalization due to the spin-fluctuation exchange is fundamental to reconcile ARPES and specific-heat measurements.

Similar conclusions are drawn from the analysis of the superfluid density at zero temperature, $J_{s,\alpha}(0)$. A simple calculation using the electronic masses extracted from the ARPES data would give $J_s(0) \approx 700$ K, much higher than the best experimental estimates give $J_s(0) \approx 300$ – 400 K [36, 37]. Such discrepancy is, however, overcome in our multiband calculations where we take into account the band

narrowing due to the electronic correlation. In this case we find $J_s(0) = \sum_\alpha J_{s,\alpha}(0) = 300$ K, once more in very good agreement with the experimental findings.

4 Conclusions

In conclusion, we showed that the band shifts reported in pnictides when comparing the experimentally measured Fermi surfaces and band dispersions with DFT calculations are a direct consequence of the coupling to a bosonic mode, once that the strong particle-hole asymmetry and the multiband character of these systems are properly taken into account. The sign of the measured shifts provides direct evidence of the predominance of the *interband* scattering, suggesting spin fluctuations as a natural candidate for such a kind of interband coupling. We also have shown that the multiband/multigap properties of the superconducting and normal state of optimally doped BKFA can consistently be explained within an intermediate-strong coupling four-band Eliashberg theory once the high-energy band renormalization observed in ARPES data, probably due to the electronic correlation, is properly taken into account.

References

- Kamihara, Y., et al.: J. Am. Chem. Soc. **128**, 10012 (2006)
- Kamihara, Y., et al.: J. Am. Chem. Soc. **130**, 3296 (2008)
- Lebègue, S.: Phys. Rev. B **75**, 035110 (2007)
- Mazin, I.I., et al.: Phys. Rev. Lett. **101**, 057003 (2008)
- Singh, D.J.: Phys. Rev. B **78**, 094511 (2008)
- Nekrasov, I.A., Pchelkina, Z.V., Sadovskii, M.V.: JETP Lett. **87**, 620 (2008)
- Nekrasov, I.A., Pchelkina, Z.V., Sadovskii, M.V.: JETP Lett. **88**, 144 (2008)
- Mazin, I.I., et al.: Phys. Rev. B **78**, 085104 (2008)
- Ding, H., et al.: [arXiv:0812.0534](https://arxiv.org/abs/0812.0534) (2008)
- Yang, L.X., et al.: Phys. Rev. Lett. **102**, 107002 (2009)
- Wray, L., et al.: Phys. Rev. B **78**, 184508 (2008)
- Yi, M., et al.: Phys. Rev. B **80**, 024515 (2009)
- Coldea, A.I., et al.: Phys. Rev. Lett. **101**, 216402 (2008)
- Carrington, A., et al.: Physica C **469**, 459 (2009)
- Analytis, J.G., et al.: Phys. Rev. Lett. **103**, 076401 (2009)
- Ding, H., et al.: Europhys. Lett. **83**, 47001 (2008)
- Lu, D.H., et al.: Nature **455**, 81 (2008)
- Lu, D.H., et al.: Physica C **469**, 452 (2009)
- Ni, N., et al.: Phys. Rev. B **78**, 014507 (2008)

20. Mu, G., et al.: Phys. Rev. B **79**, 174501 (2009)
21. Kant, Ch., et al.: Phys. Rev. B **81**, 014529 (2010)
22. Ortenzi, L., et al.: Phys. Rev. Lett. **103**, 046404 (2009)
23. Benfatto, L., Cappelluti, E., Castellani, C.: Phys. Rev. B **80**, 214522 (2009)
24. Millis, A.J.: Phys. Rev. B **45**, 13047 (1992)
25. Qazilbash, M.M., et al.: Nat. Phys. **5**, 647 (2009)
26. Aichhorn, M., et al.: Phys. Rev. B **80**, 085101 (2009)
27. Skornyakov, S.L., et al.: Phys. Rev. B **80**, 092501 (2009)
28. Yang, W.L., et al.: Phys. Rev. B **80**, 014508 (2009)
29. McQueen, T.M., et al.: Phys. Rev. B **78**, 024521 (2008)
30. Analytis, J.G., et al.: [arXiv:0810.5368](https://arxiv.org/abs/0810.5368) (2008)
31. Kohama, Y., et al.: J. Phys. Soc. Jpn. **77**, 094715 (2008)
32. Dolgov, O.V., et al.: Phys. Rev. B **79**, 060502 (2009)
33. Ummarino, G.A., et al.: Phys. Rev. B **80**, 172503 (2009)
34. Evtushinsky, D.V., et al.: New J. Phys. **11**, 055069 (2009)
35. Ma, F., Lu, Z.-Y., Xiang, T.: [arXiv:0806.3526](https://arxiv.org/abs/0806.3526) (2008)
36. Hiraishi, M., et al.: J. Phys. Soc. Jpn. **78**, 023710 (2009)
37. Li, G., et al.: Phys. Rev. Lett. **101**, 107004 (2008)